Visible-Light-Response and Photocatalytic Activities of TiO_2 and $SrTiO_3$ Photocatalysts Codoped with Antimony and Chromium

Hideki Kato and Akihiko Kudo*

Department of Applied Chemistry, Faculty of Science, Science University of Tokyo, 1-3 Kagurazaka, Shinjuku-ku, Tokyo 162-8601, Japan

Received: January 24, 2002; In Final Form: March 20, 2002

TiO_2 and $SrTiO_3$ codoped with antimony and chromium showed intense absorption bands in the visible light region and possessed 2.2 and 2.4 eV of energy gaps, respectively. TiO_2 codoped with antimony and chromium evolved O_2 from an aqueous silver nitrate solution under visible light irradiation, while $SrTiO_3$ codoped with antimony and chromium evolved H_2 from an aqueous methanol solution. The activity of TiO_2 photocatalyst codoped with antimony and chromium was remarkably higher than that of TiO_2 doped with only chromium. It was due to that the charge balance was kept by codoping of Sb^{5+} and Cr^{3+} ions, resulting in the suppression of formation of Cr^{6+} ions and oxygen defects in the lattice which should work as effectively nonradiative recombination centers between photogenerated electrons and holes.

1. Introduction

It has been reported that some metal oxides show reasonable activities for water splitting into H_2 and O_2 in a stoichiometric ratio under UV irradiation.[1,2] However, these photocatalysts are not appropriate for the solar light energy conversion. On the other hand, it has been also reported that some metal oxides and sulfides are visible-light-driven photocatalysts for H_2 evolution[3−6] or O_2 evolution[6−9] from water involving sacrificial reagents. Recently, Zou and Arakawa and co-workers have reported the water splitting into H_2 and O_2 under visible light irradiation using $NiO_X/In_{0.9}Ni_{0.1}TaO_4$.[10] However, the highly efficient photocatalyst for water splitting under visible light irradiation has not been developed yet.

The doping of a foreign element into active photocatalysts with wide band gaps in order to make a donor or an acceptor level in the forbidden band is one of the ways to develop new visible-light-driven photocatalysts. There are many reports that the doped photocatalysts and semiconductor electrodes, such as TiO_2,[11−15] $SrTiO_3$,[16−18] and ZnS,[4,5] respond to visible light. In particular, the effects of doping of Cr^{3+} ions into TiO_2 and $SrTiO_3$ on the photocurrent of semiconductor electrodes[16−18] and the photocatalytic decomposition of organic compounds[11,12] have been widely studied. Although Cr^{3+}-doped TiO_2 and $SrTiO_3$ certainly possess visible light response, the photocurrent and photocatalytic activities are remarkably decreased in comparison with those of nondoped TiO_2 and $SrTiO_3$ even under band gap excitation[11,16,17] As far as the authors know, there are no reports for efficient photocatalytic H_2 or O_2 evolution from water over TiO_2 and $SrTiO_3$ doped with Cr^{3+} ions. When Cr^{3+} ions were partly substituted for Ti^{4+} ions in titanates, oxygen defects and/or Cr^{6+} ions should be formed to keep the charge balance, and they may cause the increase in the recombination centers between photogenerated electrons and holes.

Rutile TiO_2 powders codoped with antimony and chromium, and antimony and nickel are well-known orange and yellow pigments, respectively. It is expected that the charge balance in the TiO_2 codoped with antimony and chromium, and antimony and nickel may be maintained without the oxygen defects and Cr^{6+} ions formation by codoping of Sb^{5+} ions.

In the present study, the effects of antimony codoping into TiO_2 and $SrTiO_3$ doped with some transition metal ions on photophysical and photocatalytic properties were investigated in order to develop new active photocatalysts for H_2 and O_2 evolution under visible light irradiation.

2. Experimental Section

Rutile TiO_2 and $SrTiO_3$ powders codoped with antimony and transition metals were prepared by conventional solid-state reactions. The starting materials (TiO_2 (Soekawa Chemical; 99.9%), $SrCO_3$ (Kanto Chemical; 99.9%), Cr_2O_3 (Kanto Chemical; 98.5%), NiO (Kanto Chemical; 99.9%), CuO (Kanto Chemical; 98.0%), and Sb_2O_3 (Nacali tesque; 98%)) were mixed in the ratio according to the composition of $Ti_{1-X-Y}Sb_XM_YO_2$ (M:Cr, Ni, and Cu, and denoted as TiO_2:Sb/M) and $SrTi_{1-X-Y}Sb_X$-Cr_YO_3 (denoted as $SrTiO_3$:Sb/Cr). The mixtures were calcined at 1420 K for 10 h for TiO_2:Sb/M and for 20−40 h for $SrTiO_3$:Sb/Cr in air using alumina crucibles (purity: 99.7%). The obtained powders were confirmed by X-ray diffraction (Rigaku; RINT-1400). Pt cocatalysts were loaded from an aqueous H_2-$PtCl_6{\cdot}6H_2O$ (Tanaka Kikinzoku; 37.55% as Pt) solution by a photodeposition method.

Photocatalytic reactions of H_2 evolution from an aqueous methanol solution (8 vol %) and O_2 evolution from an aqueous silver nitrate solution (0.05 mol L^{-1}) were carried out in a gas-closed circulation system. The photocatalyst powder (0.5 g) was dispersed in a solution (320 mL) by a magnetic stirrer in a cell with a side-window made of Pyrex. The light source was an ozone free 300 W Xe illuminator (ILC technology; CERMAX-LX300F) attached with a cutoff filter to control the wavelength of the incident light. The amounts of H_2 and O_2 evolved were determined using gas chromatography (Shimadzu; GC-8A, TCD, Ar carrier).

Diffuse reflection spectra were obtained using a UV−vis−NIR spectrometer (Jasco; UbestV-570) and were converted from reflection to absorbance by the Kubelka−Munk method. Pho-

* To whom correspondence should be addressed. FAX: +81-33235-2214. E-mail: a-kudo@ch.kagu.sut.ac.jp.

10.1021/jp0255482 CCC: $22.00
Published on Web 04/23/2002

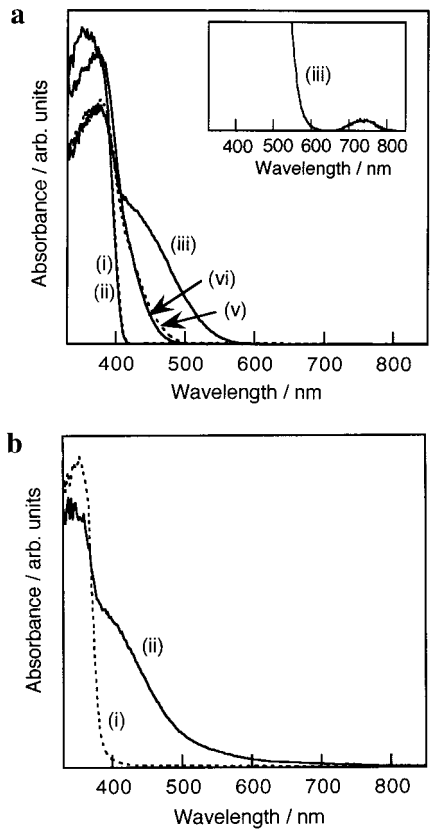

Figure 1. (a) Diffuse reflection spectra of (i) nondoped TiO_2, (ii) TiO_2 doped with Sb(3.45%), TiO_2 codoped with (iii) Sb(1.25%)/Cr(0.5%), (iv) Sb(1.25%)/Ni(0.5%), and (v) Sb(1.25%)/Cu(0.5%). The inset shows the magnification of (iii). (b) Diffuse reflection spectra of (i) nondoped $SrTiO_3$ and (ii) $SrTiO_3$ codoped with Sb(2.5%)/Cr(2%).

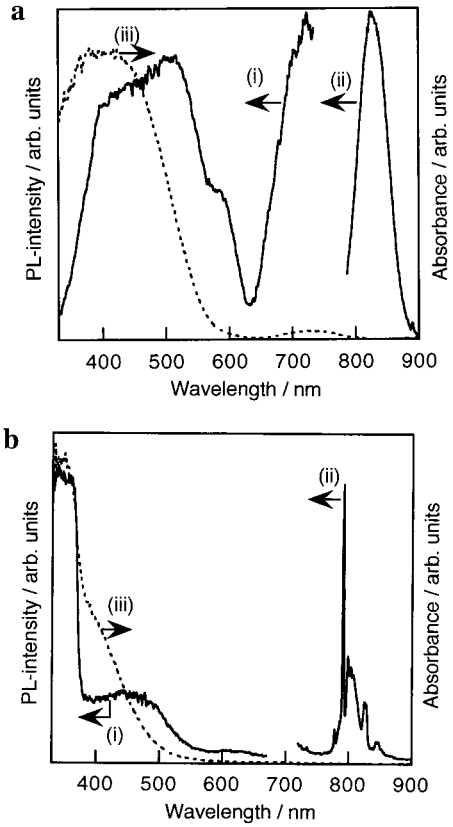

Figure 2. (a) Photoluminescence spectra of TiO_2:Sb(3.45%)/Cr-(2.3%): (i) an excitation spectrum monitored at 828 nm and (ii) an emission spectrum excited at 500 nm at 77 K, and (iii) diffuse reflection spectrum at 300 K. (b) Photoluminescence spectra of $SrTiO_3$:Sb(5%)/Cr(2%): (i) an excitation spectrum monitored at 790 nm and (ii) an emission spectrum excited at 350 nm at 77 K, and (iii) diffuse reflection spectrum at 300 K.

toluminescence was measured in vacuo at 77 K using a spectrofluorometer (Spex; FluoroMax). X-ray photoelectron spectra (XPS) were measured using an X-ray photoelectron spectrometer (Shimadzu; ESCA-3200). Elemental analyses were carried out using an X-ray spectrofluorometer (JEOL; JSX-3200).

3. Results and Discussion

3.1. Photophysical Properties of TiO_2:Sb/M (M:Cr, Ni, and Cu) and $SrTiO_3$:Sb/Cr. Parts a and b of Figure 1 show diffuse reflection spectra of TiO_2:Sb(1.25%)/M(0.5%) and $SrTiO_3$:Sb(2.5%)/Cr(2%), respectively. All TiO_2:Sb/M showed absorption bands due to a $M^{n+} \rightarrow Ti^{4+}$ charge-transfer transition in the visible light region.[12] Moreover, TiO_2:Sb/Cr also showed a weak absorption band at 650−800 nm due to a d−d transition $^4A_2 \rightarrow {}^4T_2$ in Cr^{3+} ions with octahedral systems as shown in an inset.[12] The orange TiO_2:Sb/Cr powder had an absorption edge at the longest wavelength among TiO_2:Sb/M (M:Cr, Ni, and Cu) powders. The energy gaps of TiO_2 codoped with Sb/Cr, Sb/Ni, and Sb/Cu were estimated to be 2.2, 2.6, and 2.6 eV from the absorption edges, respectively. It indicated that Cr^{3+} ions made a donor level at more negative position in the forbidden band than Ni^{2+} and Cu^{2+} ions. The absorption band in the visible light region due to the $Cr^{3+} \rightarrow Ti^{4+}$ charge-transfer transition was also observed in $SrTiO_3$:Sb/Cr as shown in Figure 1b.[16] Absorption spectra of TiO_2 and $SrTiO_3$ codoped with Sb/Cr were similar to those of TiO_2[11,12] and $SrTiO_3$[16,17] doped with only Cr^{3+} ions. Moreover, TiO_2 doped with only antimony showed the same absorption spectrum as nondoped TiO_2. Therefore, the doped transition metal ions play an important role for the absorption bands observed in the visible light region for TiO_2 and $SrTiO_3$ codoped with antimony and transition metals.

TiO_2 and $SrTiO_3$ codoped with antimony and chromium showed photoluminescence of Cr^{3+} ions at 77 K. Parts a and b of Figure 2 show the photoluminescence spectra and diffuse reflection spectrum of TiO_2:Sb(3.45%)/Cr(2.3%) and $SrTiO_3$:Sb(5%)/Cr(2%), respectively. TiO_2:Sb/Cr showed a broad emission band at 828 nm. It was similar to the emission of Cr^{3+} ions doped into $Sr_XBa_{1-X}Nb_2O_6$ ascribed to the d−d transition $^2T_2 \rightarrow {}^4A_2$ in Cr^{3+} ions.[19] The emission was observed by excitation of the $Cr^{3+} \rightarrow Ti^{4+}$ charge-transfer transition and the d−d transition $^4A_2 \rightarrow {}^4T_2$ bands while no emission was observed by the band gap excitation ($\lambda < 400$ nm) of the TiO_2 host. It indicated that the photogenerated holes in the valence band (O2p) of TiO_2 were not able to transfer to Cr^{3+} ions of emission centers. On the other hand, $SrTiO_3$:Sb/Cr showed the ruby-line emission (the d−d transition $^2E \rightarrow {}^4A_2$) at 790 nm. It has been reported that $SrTiO_3$ doped with only Cr^{3+} ions also shows the ruby-line emission at the same wavelength as $SrTiO_3$:Sb/Cr.[20] The wavelengths of the ruby-line emission of $SrTiO_3$:Sb/Cr and $SrTiO_3$:Cr were longer than those of other materials such as Al_2O_3:Cr (693 nm)[21] and $KTaO_3$:Cr,Li (745 nm).[22] The ruby-line emission of $SrTiO_3$:Sb/Cr was observed by excitation of not only the $Cr^{3+} \rightarrow Ti^{4+}$ charge-transfer transition band but also the band gap of the $SrTiO_3$ host. It indicated that photogenerated holes in the valance band of $SrTiO_3$ were able to transfer easily to Cr^{3+} ions of emission centers. Thus, the

TABLE 1: Photocatalytic Activities of Sb/M-Doped TiO_2 and Sb/Cr-Doped $SrTiO_3$ Powder[a]

host catalyst	dopant (mol % to Ti)	energy gap/eV	incident light/nm	activity/μmol h^{-1} H_2[b]	activity/μmol h^{-1} O_2[c]
TiO_2 (rutile)	none	3.0	>300	21[d]	357
	Cr(2.3)		>300		0
	Sb(1.25)/Cr(0.5)	2.2	>420	0.06[d]	31.5
	Sb(2.4)/Cr(1.0)	2.2	>300	0.65[d]	44.8
	Sb(1.25)/Ni(0.5)	2.6	>420	0[d]	12.8
	Sb(1.25)/Cu(0.5)	2.6	>420	0.08[d]	5.5
$SrTiO_3$	none	3.2	>300	139[e]	114
	Sb(2.5)/Cr(2)	2.4	>300	102[f]	0.9
	Sb(2.5)/Cr(2)	2.4	>420	78[f]	0.9

[a] Catalyst: 0.5 g. Reactant solution: 320 mL. Light source: 300 W Xe lamp. Cell: side irradiation type. [b] From 8 vol % aqueous methanol solution. [c] From 0.05mol L^{-1} aqueous silver nitrate solution. [d] Pt (1 wt %) was loaded. [e] Pt (0.2 wt %) was loaded. [f] Pt (0.3 wt %) was loaded.

photoluminescence property of the $SrTiO_3$:Sb/Cr was different from that of TiO_2:Sb/Cr.

3.2. Photocatalytic Activities of TiO_2:Sb/Cr and $SrTiO_3$:Sb/Cr under Visible Light Irradiation. Table 1 shows photocatalytic activities of TiO_2:Sb/M (M:Cr, Ni, and Cu) and $SrTiO_3$:Sb/Cr. TiO_2:Sb/M hardly evolved H_2 from an aqueous methanol solution but showed activities for O_2 evolution from an aqueous silver nitrate solution under visible light irradiation. TiO_2:Sb/Cr showed the highest activity among them. The number of absorbed photons of TiO_2:Sb/Cr should be larger than those of TiO_2:Sb/Ni and TiO_2:Sb/Cu because of the smallest band gap. It was considered that the order of photocatalytic activities of TiO_2:Sb/M was mainly due to the number of absorbed photons. The reasons why the H_2 evolution activity of TiO_2:Sb/Cr was negligible were considered as follows. Crystal structures of prepared TiO_2:Sb/M were rutile of which abilities for H_2 evolution were low. Moreover, the position of conduction bands of TiO_2:Sb/M might slightly shift to lower level due to adulteration of excitation levels of transition metal ions.

$SrTiO_3$:Sb/Cr evolved H_2 from an aqueous methanol solution under visible light irradiation being different from TiO_2:Sb/Cr as shown in Table 1. It was due to the higher conduction band level of $SrTiO_3$ than rutile TiO_2. However, the activity of $SrTiO_3$:Sb/Cr for O_2 evolution under visible light irradiation was very low. The activity for O_2 evolution was not increased even by the band gap excitation under UV light irradiation.

When photocatalyst materials are doped with transition metal ions with a partially filled d-orbital, they usually lose their photocatalytic activities even under the band gap excitation of the host materials. In fact, TiO_2 doped with only chromium showed no activities in the present study. In contrast, the activities of Sb/Cr codoped TiO_2 for O_2 evolution and $SrTiO_3$ for H_2 evolution were still active under the band gap excitation. Especially, H_2 evolution on the $SrTiO_3$:Sb/Cr was not suppressed so much compared to that on nondoped $SrTiO_3$. It indicated that the codoped antimony contributed to maintaining the photocatalytic activities by band gap excitation. The photocatalytic properties of the Sb/Cr codoped titanate photocatalysts depended on the host materials. It was mainly due to characteristic of doped Cr^{3+} ions depending on the host materials, and it was also observed in the photoluminescence properties as shown in Figure 2a,b.

Figure 3 shows an action spectrum for O_2 evolution from an aqueous silver nitrate solution over the TiO_2:Sb(5.75%)/Cr(2.3%) photocatalyst. The horizontal axis indicates the cutoff wavelength at which transmittance is almost 0%. The action

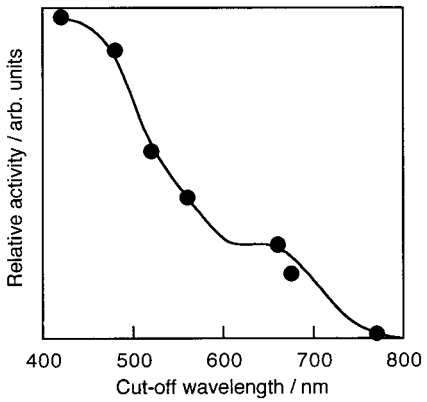

Figure 3. An action spectrum for O_2 evolution from an aqueous silver nitrate solution over TiO_2:Sb(5.75%)/Cr(2.3%) photocatalyst. Catalyst: 0.5 g, an aqueous silver nitrate solution: 0.05 mol L^{-1}, 320 mL, 300 W Xe lamp ($\lambda \geq 420$ nm), side irradiation cell.

spectrum agreed well to the diffuse reflection spectra shown in Figures 1a and 2a. It was revealed that the TiO_2:Sb/Cr photocatalyst was able to use the wide range in the visible light region ($\lambda \leq 680$ nm).

3.3. Schemes of Photoluminescence and Photocatalytic Reactions of TiO_2:Sb/Cr and $SrTiO_3$:Sb/Cr. The schemes of photoluminescence and photocatalytic reactions on TiO_2:Sb/Cr and $SrTiO_3$:Sb/Cr derived from the results are shown in Figure 4. It has been reported that the photoluminescence of Cr^{3+} ions depends on the interaction of Cr^{3+} ions.[21] Isolated Cr^{3+} ions show the sharp-line emission, while Cr^{3+} ions interacting with each other and/or other ions such as O^{2-} show the broad emission band in the long wavelength side. Therefore, the broad emission band observed for TiO_2:Sb/Cr in the near-infrared region indicated that Cr^{3+} ions doped in TiO_2 made an electron donor band. In contrast, Cr^{3+} ions doped in $SrTiO_3$ would form not a band but a discrete level. It was considered that difference in the characteristics of Cr^{3+} ions doped in TiO_2 and $SrTiO_3$ would be due to the crystal structures of the host materials (edge or corner sharing of TiO_6 units).

When UV light was irradiated on TiO_2:Sb/Cr, electrons and holes were generated in the conduction and valence bands of TiO_2:Sb/Cr by band gap excitation, respectively. Although holes would travel in the valence band, the holes were not able to transfer to Cr^{3+} ions (Figure 4a). In the photocatalytic reactions, the electrons in the conduction band were hardly able to reduce water to H_2 because of the low potential of the conduction band (Figure 4b). In contrast, the holes in the valence band were able to oxidize water to form O_2. On the other hand, when visible light was irradiated on TiO_2:Sb/Cr, electrons and holes were generated in the conduction band and the electron donor band consisting of Cr^{3+} (and/or O^{2-}) ions, respectively (Figure 4c). The holes in the donor band would have the large mobility because of the interaction of Cr^{3+} ions. Then, electrons and holes would recombine by accompanied with the broad emission as shown in Figure 2a. The holes in the donor band were able to oxidize water as well as holes in the valence band (Figure 4d). In the case of $SrTiO_3$:Sb/Cr, electrons and holes were generated in conduction and valence bands under UV light irradiation, respectively. The holes in the valence band would transfer to Cr^{3+} ions of emission centers (Figure 4e) being different from UV light-irradiated TiO_2:Sb/Cr. In the photocatalytic reactions, electrons in the conduction band were able to reduced water to H_2 (Figure 4f). The potential of the donor level consisting of Cr^{3+} ions in $SrTiO_3$:Sb/Cr was estimated to be 2.2 eV from the energy gap (2.4 eV) and the conduction band level of $SrTiO_3$

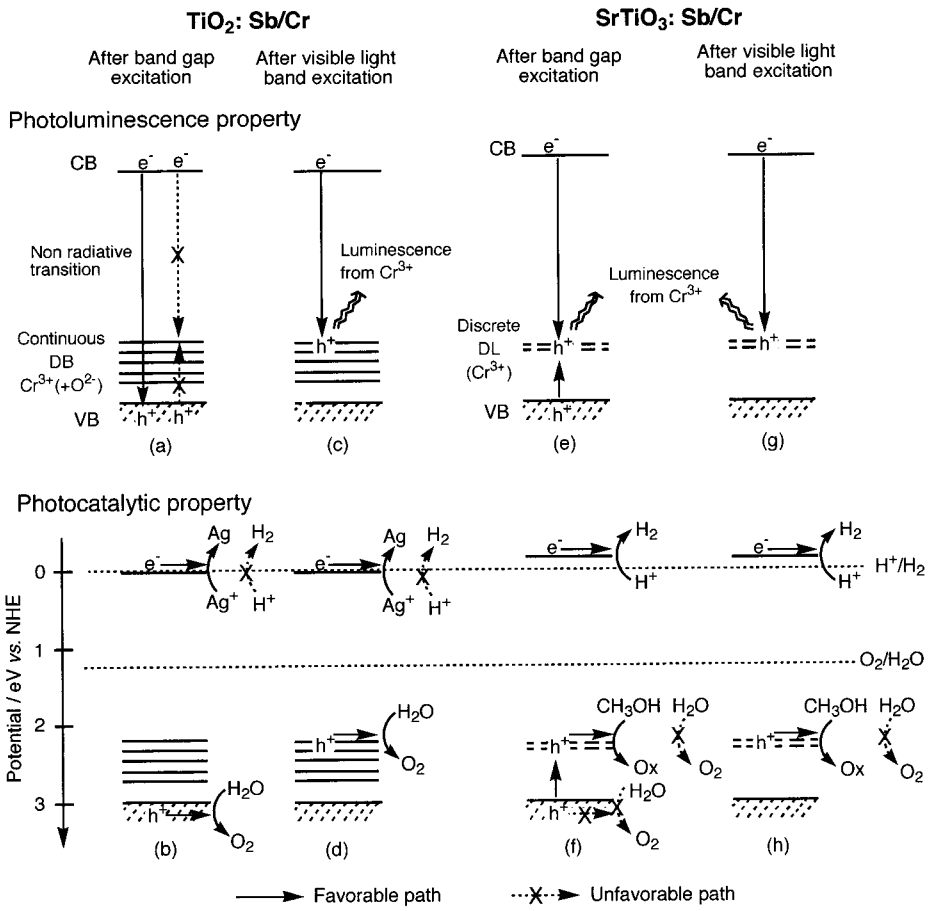

Figure 4. Schemes of photoluminescence and photocatalytic reactions on TiO_2:Sb/Cr and $SrTiO_3$:Sb/Cr.

(−0.2 eV). The donor level was close to that of TiO_2:Sb/Cr. The potential would have been thermodynamically enough for oxidation of water to form O_2. However, the mobility of holes in the donor level consisting of Cr^{3+} ions seemed to be small because the donor level in the forbidden band of $SrTiO_3$ was not continuous and did not form the band as described above, resulting in that O_2 evolution accompanied with a 4-electrons oxidation reaction hardly proceeded. In contrast, the holes in such donor levels would be able to promote easy reactions such as the methanol oxidation. On the other hand, electrons and holes were also generated in the conduction band and the donor level by visible light irradiation, respectively (Figure 4g,h). Therefore, visible light-irradiated $SrTiO_3$:Sb/Cr showed the similar photoluminescence and photocatalytic properties to UV light-irradiated $SrTiO_3$:Sb/Cr.

3.4. Role of Antimony Codopant. The X-ray diffraction patterns of TiO_2 and $SrTiO_3$ codoped with antimony and transition metal ions were the same as those of nondoped TiO_2 and $SrTiO_3$, respectively, except for small shifts. It indicated that antimony and transition metal ions were substituted for Ti^{4+} ion sites. X-ray diffraction peaks around 36° in two theta of TiO_2 codoped with chromium (2.3%) and various amount of antimony are shown in Figure 5. The diffraction peaks of TiO_2 codoped in the ratio of Sb/Cr < 1 were slightly shifted to higher angles compared to that of nondoped TiO_2, suggesting the substitution of Cr^{6+} (0.44 Å) and Sb^{5+} (0.60 Å) for Ti^{4+} (0.605 Å).[23] The diffraction peak of TiO_2 codoped in the ratio of Sb/Cr = 1 was hardly changed, suggesting the substitution of Cr^{3+} (0.615 Å) and Sb^{5+} for Ti^{4+}.[23] The diffraction peaks of TiO_2 codoped in the ratio of Sb/Cr >1 were shifted to lower angles as the ratio of Sb/Cr was increased. In these materials, Sb^{3+} with a large ionic radius (0.76 Å)[23] had to be substituted more

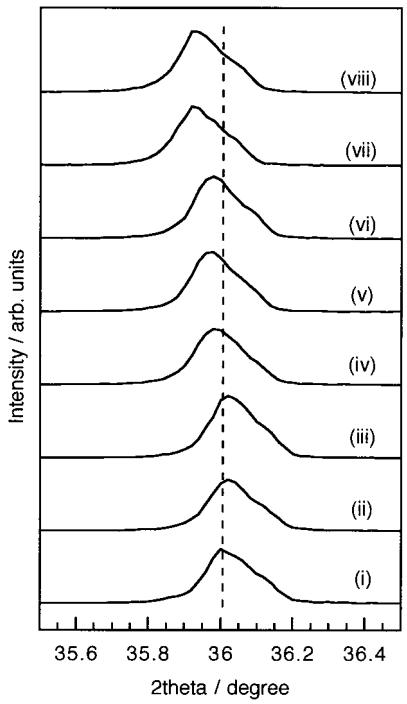

Figure 5. X-ray diffraction peaks of TiO_2:Sb(X%)/Cr(2.3%); (i) nondoped, (ii) Sb/Cr = 0, (iii) Sb/Cr = 0.5, (iv) Sb/Cr = 1, (v) Sb/Cr = 1.5, (vi) Sb/Cr = 2, (vii) Sb/Cr = 2.5, and (viii) Sb/Cr = 3.5.

or less. However, the shift was no longer observed between TiO_2 codoped in the ratio Sb/Cr = 2.5 and 3.5. Table 2 shows results of elemental analyses by XRF for TiO_2:Sb/Cr photocatalysts. Although the amounts of chromium after calcination

TABLE 2: Elemental Analyses by X-ray Fluorescence for TiO_2:Sb/Cr Photocatalysts

ratio of Sb to Cr	amount of dopant/mol % to Ti			
	weighed amounts in starting materials		analyzed amount after calcination	
	Cr	Sb	Cr	Sb
0	2.3	0	2.5	0
0.5	2.3	1.15	2.5	1.1
1.0	2.3	2.3	2.5	2.1
1.5	2.3	3.45	2.5	3.1
2.0	2.3	4.6	2.5	3.4
2.5	2.3	5.75	2.5	4.4
3.5	2.3	8.05	2.7	4.4

were almost the same as those in starting materials, the amounts of antimony of TiO_2:Sb/Cr were decreased by calcination. The larger the ratio of Sb/Cr, the larger the degree of the antimony loss became. The amount of antimony in TiO_2 codoped in the ratio of Sb/Cr = 2.5 was the same as that of Sb/Cr = 3.5. It was due to volatilization of the excess amount of antimony over the limitation of the doping amount.

The oxidation numbers of doped antimony and chromium were investigated by XPS. Parts a and b of Figure 6 show the Cr2p and Sb4d of XPS of TiO_2:Sb/Cr, respectively. TiO_2 doped with only chromium (Sb/Cr = 0) showed not only a large peak assigned to trivalent chromium at 576.7 eV but also a shoulder peak assigned to hexavalent chromium at 579.2 eV. When antimony was codoped in the ratios of Sb/Cr = 1 and 1.5, only large peaks due to the trivalent chromium were observed. On the other hand, TiO_2 codoped in the ratio of Sb/Cr = 1 showed a large peak assigned to pentavalent antimony at 36.7 eV with a shoulder peak assigned to trivalent antimony. When antimony was codoped in the ratio of Sb/Cr = 1.5, the peak intensity of trivalent antimony was the same as that of pentavalent antimony. Thus, the oxidation numbers of antimony and chromium codoped into TiO_2 were clarified by XPS measurements, and it supported the shifts observed in XRD.

Diffuse reflection spectra of TiO_2 codoped with chromium (2.3%) and various amounts of antimony are shown in Figure 7. The color of TiO_2:Sb/ Cr powders depended on the amounts of codoped antimony. TiO_2:Sb/Cr powders were black when the amounts of codoped antimony were smaller than that of doped chromium (Sb/Cr < 1). The color of TiO_2:Sb/Cr powders was turned into orange when the amounts of codoped antimony were equal to or larger than that of doped chromium (Sb/Cr ≥ 1). If TiO_2 doped with Cr^{3+} ions was prepared by a solid-state reaction in air, Cr^{6+} ions were partly formed due to the charge balance in the TiO_2 lattice, resulting in being black. The orange TiO_2:Cr^{3+} powder was able to be obtained by reduction of the black TiO_2:Cr^{3+}/Cr^{6+} powder by H_2. However, the oxygen defects should be formed in the orange TiO_2:Cr^{3+} powder to keep the charge balance, and the stoichiometry would be according to the composition of $Ti^{IV}_{1-2X}Cr^{III}_{2X}O_{2-X}$. In contrast, when antimony was codoped with Cr^{3+} ions, the TiO_2:Sb/Cr would not require the formation of not only Cr^{6+} ions but also oxygen defects because the charge balance was kept by Sb^{5+} ions. When the excess amount of antimony was codoped, the charge balance would be kept by the coexistence of Sb^{5+} and Sb^{3+} ions according to the composition of $Ti^{IV}_{1-2X-2Y}Sb^{V}_{X+Y}$-$Sb^{III}_{Y}Cr^{III}_{X}O_2$: it was supported by XPS. Thus, it was found that the Cr^{3+}-doped TiO_2 powder without any oxygen defects and Cr^{6+} formation was easily obtained by codoping of antimony.

The photocatalytic activities of TiO_2:Sb/Cr for O_2 evolution from an aqueous silver nitrate solution strongly depended on the ratio of antimony to chromium as shown in Figure 8. The oxygen evolution was observed over the orange TiO_2:Sb/Cr

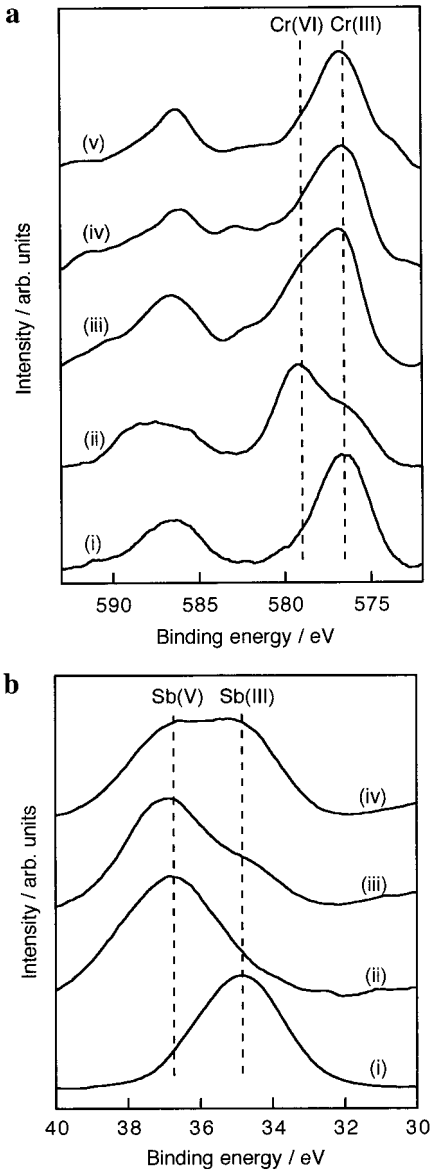

Figure 6. (a) X-ray photoelectron spectra of Cr2p of TiO_2:Sb(X%)/Cr(2.3%): (i) Cr_2O_3, (ii) CrO_3, (iii) Sb/Cr = 0, (iv) Sb/Cr = 1, and (v) Sb/Cr = 1.5. (b) X-ray photoelectron spectra of Sb4d of TiO_2:Sb(X%)/Cr(2.3%): (i) Sb_2O_3, (ii) Sb_2O_5, (iii) Sb/Cr = 1, and (iv) Sb/Cr = 1.5.

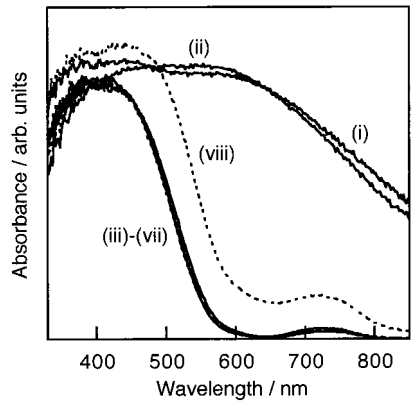

Figure 7. Diffuse reflection spectra of TiO_2:Sb(X%)/Cr(2.3%): (i) Sb/Cr = 0, (ii) Sb/Cr = 0.5, (iii) Sb/Cr = 1, (iv) Sb/Cr = 1.5, (v) Sb/Cr = 2, (vi) Sb/Cr = 2.5, (vii) Sb/Cr = 3.5, and (viii) hydrogen-reduced (i).

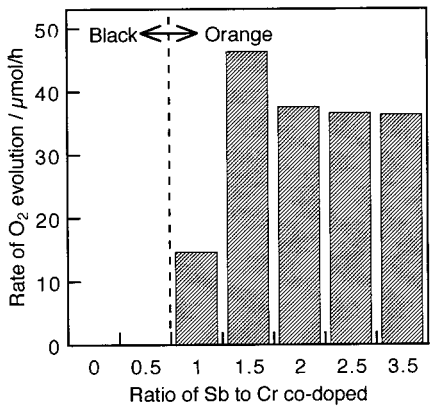

Figure 8. Dependence of Photocatalytic activity of TiO_2:Sb(X%)/Cr-(2.3%) upon the ratio of antimony to chromium. Catalyst: 0.5 g, an aqueous silver nitrate solution: 0.05 mol L^{-1}, 320 mL, 300 W Xe lamp ($\lambda \geq 420$ nm), side irradiation cell.

powders in the ratio of Sb/Cr ≥ 1, while no oxygen was evolved over the black TiO_2:Sb/Cr powders in the ratio of Sb/Cr < 1. The highest activity was obtained when antimony and chromium were codoped in the ratio of Sb/Cr $= 1.5$. The activities of TiO_2:Sb/Cr in the ratios of Sb/Cr $= 2$, 2.5, and 3.5 were slightly smaller than those in the ratio of Sb/Cr $=1.5$ but 2.5 times higher than those in the ratio of Sb/Cr $= 1$. Cr^{6+} ions would be partly formed in the black TiO_2:Sb/Cr as described above. It was considered that Cr^{6+} would work as effectively nonradiative recombination centers between photogenerated electrons and holes, resulting in no activities. Moreover, the TiO_2:Cr^{3+} prepared by H_2 reduction also showed no activities despite the appearance of orange color. It was due to oxygen defects which would also work as effectively nonradiative recombination centers. Thus, the recombination was dominant in the TiO_2 doped with only chromium: it was supported by the photoluminescent property that no emission was observed in the TiO_2:Cr. In contrast, the formation of such nonradiative centers would be suppressed in the orange TiO_2:Sb/Cr by codoping of antimony as mentioned above, resulting in the appearances of photocatalytic activities. It was considered that codoped Sb^{5+} ions would be located close to Cr^{3+} ions in the lattice to compensate for the charge balance. Although the stoichiometry of Sb^{5+}/Cr^{3+} to keep the charge balance is unity, the photocatalytic activity of TiO_2:Sb/Cr in the ratio of Sb/Cr $= 1$ was less than that in the ratio Sb/Cr ≥ 1.5. It was clarified from XRF and XPS measurement that the ratio of Sb^{5+}/Cr^{3+} was less than unity in the TiO_2:Sb/Cr in the ratio of Sb/Cr $= 1$ because of the volatilization of antimony and the formation of Sb^{3+} ions. Therefore, it was considered that a few oxygen defects were formed in TiO_2:Sb/Cr in the ratio of Sb/Cr $= 1$ to keep the charge balance, but not formed in the ratio of Sb/Cr ≥ 1.5. It is the main reason that the activities of TiO_2:Sb/Cr in the ratio of Sb/Cr ≥ 1.5 were higher than those in the ratio of Sb/Cr $= 1$.

Codoping of elements to keep the charge balance is one of the effective ways to develop highly active TiO_2 photocatalysts with response to visible light by doping of transition metals. Antimony is one of the desirable codopants for titanate photocatalysts because of the facility for taking trivalent and pentavalent states. The stoichiometry of the antimony codoping would not be severe, because of excess amount of antimony would keep the charge balance by themselves.

4. Conclusions

(1) TiO_2 codoped with antimony and transition metals (chromium, nickel, and copper) and $SrTiO_3$ codoped with antimony and chromium showed the intense absorption bands in the visible light region. It was found that the TiO_2 and $SrTiO_3$ codoped with antimony and chromium were new visible-light-driven photocatalysts for O_2 evolution from an aqueous silver nitrate solution and H_2 evolution from an aqueous methanol solution, respectively.

(2) TiO_2:Sb/Cr showed the broad emission at 828 nm owing to the d−d transition $^4T_2 \rightarrow {}^4A_2$ in Cr^{3+} ions by excitation of the $Cr^{3+} \rightarrow Ti^{4+}$ charge transfer and the d−d transition $^4A_2 \rightarrow {}^4T_2$ in Cr^{3+} ions. $SrTiO_3$:Sb/Cr showed the ruby-line emission at 790 nm owing to d−d transition $^2E \rightarrow {}^4A_2$ in Cr^{3+} ions by excitation of the band gap of $SrTiO_3$ and the $Cr^{3+} \rightarrow Ti^{4+}$ charge transfer. The photoluminescence properties of Cr^{3+} ions in codoped TiO_2 and $SrTiO_3$ with antimony and chromium depended on the interaction of Cr^{3+} ions with each other and/or O^{2-} owing to the crystal structures of host materials.

(3) The photocatalytic activity of antimony and chromium-*co*-doped TiO_2 was higher than that of doped with only chromium. It was clarified from XPS measurement that high activities of codoped TiO_2 and $SrTiO_3$ were due to the keeping of the charge balance by codoped Sb^{5+} ions.

Acknowledgment. The authors thank Prof. K. Domen (Research Laboratory of Resources Utilization, Tokyo Institute of Technology) for XPS measurement. This work was supported by Core Research for Evolutional Science and Technology (CREST). One of us (H.K.) has been awarded a Research Fellowship of the Japan Society for the Promotion of Science for Young Scientists.

References and Notes

(1) Domen, K.; Kondo, J. N.; Hara, M.; Takata, T. *Bull. Chem. Soc. Jpn.* **2000**, *73*, 1307 and references therein.

(2) Kudo, A. *J. Ceram. Soc. Jpn.* **2001**, *109*, S81 and references therein.

(3) Sakata, T. Heterogeneous Photocatalysis at Liquid−Solid Interfaces. In *Photocatalysis*; Serpone, N., Pelizzetti, E., Edd.; Wiley: New York, 1989; Chapter 10, pp 311−338.

(4) Kudo, A.; Sekizawa, M. *Catal. Lett.* **1999**, *58*, 241.

(5) Kudo, A.; Sekizawa, M. *Chem. Commun.* **2000**, 1371.

(6) Yoshimura, J.; Ebina, Y.; Kondo, J.; Domen, K.; Tanaka, A. *J. Phys. Chem.* **1993**, *97*, 1970.

(7) Darwent, J. R.; Mills, A. *J. Chem. Soc., Faraday. Trans. 2* **1982**, *78*, 359.

(8) Ohno, T.; Tanigawa, F.; Fujihara, K.; Izumi, S.; Matsumura, M. *J. Photochem. Photobiol. A: Chem.* **1999**, *127*, 107.

(9) Kudo, A.; Omori, K.; Kato, H. *J. Am. Chem. Soc.* **1999**, *121*, 11459.

(10) Zou, Z.; Ye, J.; Sayama, K.; Arakawa, H. *Nature* **2001**, *414*, 625.

(11) Herrmann, J.-M.; Disdier, J.; Pichat, P. *Chem. Phys. Lett.* **1984**, *108*, 618.

(12) Serpone, N.; Lawless, D. *Langmuir* **1994**, *10*, 643.

(13) Sakata, Y.; Yamamoto, T.; Okazaki, T.; Imamura, H.; Tsuchida, S. *Chem. Lett.* **1998**, 1253.

(14) Iwasaki, M.; Hara, M.; Kawada, H.; Toda, H.; Ito, S. *J. Colloid Interface Sci.* **2000**, *224*, 202.

(15) Asahi, R.; Morikawa, T.; Ohwaki, T.; Aoki, K.; Taga, Y. *Science* **2001**, *293*, 269.

(16) Campet, G.; Dare-Edwards, M. P.; Hamnett, A.; Goodenough, J. B. *Nouv. J. Chim.* **1980**, *4*, 501.

(17) Mackor, A.; Blasse, G. *Chem. Phys. Lett.* **1981**, *77*, 6.

(18) Lam, R. U. E. t.; Haart, L. G. J. d.; Wiersma, A. W.; Blasse, G.; Tinnemans, A. H. A.; Mackor, A. *Mater. Res. Bull.* **1981**, *16*, 1593.

(19) Gao, M.; Kapphan, S.; Pankrath, R. *J. Phys. Chem. Solids* **2000**, *61*, 1959.

(20) Basun, S. A.; Bianchi, U.; Bursian, V. E.; Kaplyanskii, A. A.; Kleemann, W.; Markovin, P. A.; Sochava, L. S.; Vikhnin, V. S. *Ferroelectrics* **1996**, *183*, 255.

(21) Tolstoi, N. A.; Shun'-fu, L.; Lapidus, M. E. *Opt. Spectrosc.* **1962**, *13*, 133.

(22) Baryshev, A. V.; Basun, S. A.; Vikhnin, V. S.; Trepakov, V. A. *Phys. Solid State* **1997**, *39*, 1941.

(23) Shannon, R. D. *Acta Crystallogr.* **1976**, *A32*, 751.